ADSORPTION OF GALLIC ACID BY TAILOR-MADE MAGNETIC METAL-CERAMIC NANOCOMPOSITES

Domenico Pirozzi[1], Michele Pansini[2], Antonello Marocco[2], Serena Esposito[3*], Gabriele Barrera[4], Paola Tiberto[4], Paolo Allia[4], Filomena Sannino[5*]

[1]*Department of Chemical Engineering, Materials and Industrial Production (DICMaPI), Laboratory of Biochemical Engineering, University of Naples "Federico II", Piazzale Tecchio, 80, 80125, Naples, Italy.*
[2]*Department of Civil and Mechanical Engineering and INSTM Research Unit, Università degli Studi di Cassino e del Lazio Meridionale, Via G. Di Biasio 43, 03043 Cassino, FR, Italy.*
[3]*Department of Applied Science and Technology and INSTM Unit of Torino – Politecnico di Torino, Corso Duca degli Abruzzi 24, 10129, Torino, Italy.*
[4]*INRiM Torino, Advanced Materials for Metrology and Life Sciences, Strada delle Cacce 91, 10143 Torino, Italy.*
[5]*Department of Agricultural Sciences, University of Naples "Federico II", Via Università 100, 80055 Portici (NA), Italy.*

Corresponding Authors:

*Prof. Filomena Sannino fsannino@unina.it
Department of Agricultural Sciences
Università di Napoli "Federico II"
Via Università 100, 80055 Portici (NA), Italy

*Prof. Serena Esposito serena_esposito@polito.it
Department of Applied Science and Technology
and INSTM Unit of Torino –24, 10129, Torino, Italy.
Politecnico, Politecnico di Torino,
Corso Duca degli Abruzzi, 24 10129 Torino, Italy

ABSTRACT

In the last years gallic acid (GA) has been used in a growing number of industrial applications, thanks to its interesting properties. Unfortunately, the consequent presence of GA in wastewaters raises significant environmental problems. In this view, two tailor-made magnetic metal-ceramic nanocomposites, obtained from zeolite A, were developed for the adsorptive separation of GA from wastewaters. Optimized configurations of the nanocomposites, to increase their adsorption capacity and stability, were obtained by suitable modification of a patented process.

The adsorption process was characterized as regards the role played by the most relevant parameters (kinetics, pH, GA concentration). The GA removal was strongly affected by pH. The experimental results suggested the interactions between GA and the nanocomposites to be based on two different mechanisms.

The adsorption kinetics were in all cases described by the pseudo second-order model. The adsorption isotherms data were satisfactorily described by the Sips model, a combination of the Langmuir and Freundlich isotherm type models.

Suitable conditions were found to achieve the GA desorption, as well as the recycle of the magnetic adsorbents. In this view, a procedure for the thermal regeneration of the exhausted adsorbent was developed on the basis of the TG and DTA analyses. In order to offer a more environmentally friendly approach, as well as to achieve a full recovery of the economically valuable GA, a procedure for the alkaline desorption was successfully developed.

Keywords: *magnetic metal ceramic nanocomposites, gallic acid, adsorption, sustainable regeneration.*

1. Introduction

In the last years, the Gallic Acid (GA), 3,4,5-trihydroxybenzoic acid, has been increasingly used in the pharmaceutical industry due to its antioxidant, anti-inflammatory, antibacterial, neuroprotective and antitumor properties (Lu et al., 2006; Al Zahrani et al., 2020). It has also been used for food preservation (Zheng et al., 2018) due to its ability to reduce the rancidity, and for anti-corrosion protection of steel surfaces (Badhani et al., 2015). Furthermore, its ability to bind proteins has been exploited to develop innovative surfaces for sensing and catalysis (Sousa et al., 2018). Moreover, GA was used in conjugation with solid materials to improve its native properties: for example, with chitosan to improve its antioxidant ability (Pasanphan et al., 2010), with gold nanoparticles (Moreno-Alvarez et al., 2010) or with PVA composites (Yang et al., 2021), to enhance its antibacterial activity.

In spite of its interesting properties, the presence of GA in wastewater is associated with significant environmental problems. First of all, GA affects the color and the smell of water. Secondarily, GA may react with chlorine, widely used as for water disinfection, forming compounds such as chloroform and haloacetic acids. These compounds can reduce the oxygen dissolved in watercourses, which is essential for the survival of aquatic organisms, and are toxic for humans, being carcinogenic, teratogenic, and mutagenic (Zhang et al., 2015). In addition, it has been shown that GA may cause hemorrhagic liposis of cerebral muscles and intracerebral hemorrhage (Hsieh et al., 2015). Many valuable studies suggest adsorption as a method for separation of organic matter from water, owing to its efficiency, intrinsic simplicity and low cost (Srivastava et al., 2009; Addorisio et al., 2010; Sannino et al., 2012; Sannino et al., 2013; Esposito et al., 2013). The adsorption offers a simple, cheap and efficient method to separate the polyphenols from the complex aqueous solutions (Addorisio et al., 2011; Pirozzi et al., 2014). So far, activated carbon, silica gel, polymeric and macroporous resins have been proposed as sorbents for phenolic compounds. However, adsorption processes may be operated or by columnar plants or in batch reactor systems under continuous stirring and both systems exhibit serious drawbacks strongly hindering their diffusion. Actually, columnar plants are subject to flow troubles arising from the necessity of avoid channeling (occurring at low package density of the adsorbent) and

high head losses (occurring at high package density of the adsorbent), whereas batch reactor systems suffer from the difficulty arising in the separation of the adsorbent, if it is a loose powder, from the liquid. Furthermore, also the regeneration of the exhausted adsorbent often is not easy and straightforward (Di Martino et al., 2015). In order to establish these issues, we have developed magnetic metal-ceramic nano-composite adsorbents, to allow a simple separation from the liquid phase by an external magnet, thus preventing the generation of contaminants such as flocculants, and making easier the reuse of the adsorbent and the disposal of the waste. To this scope, tailor-made nanocomposites have been produced. Zeolite precursor have been adopted, to exploit peculiar properties of zeolites, such as high cation exchange capacity, swelling, and wide availability. The magnetic nano-composite adsorbents have been obtained by suitable modification of a patented process (Esposito et al., 2015; Esposito et al., 2018; Pansini et al., 2018) following a two-step procedure. First, commercial zeolites were exchanged with Fe^{2+} ions. Subsequently, the heavy-metal cation-exchanged zeolites underwent a thermal treatment at relatively mild temperatures (500-900 °C range) under a reducing atmosphere (2.0 vol.% H_2 in Ar). After the thermal treatment, the original zeolite structure was almost totally destroyed to obtain a dispersion of metallic Fe^0 nanoparticles in a mostly amorphous matrix of silica and alumina. Consequently, the physical-chemical properties of the nanocomposite were significantly different from those of the parent zeolite. Yet, the nanocomposite exhibited a residual porosity (Esposito et al., 2018), which is a remnant of the parent zeolite structure, that may have an impact on its applications as adsorbent. In addition, the silanol groups of the nanocomposites, also a remnant of the parent zeolite, may act as Bronsted sites, ensuring favourable interactions for adsorption processes. The proposed procedure of production of magnetic nanocomposites is very simple and cheap, and easily scalable. Similar nanocomposites have so far been tested in biochemical and environmental applications (Pansini et al., 2018; Marocco et al., 2019; Pansini et al., 2017; Esposito et al., 2020; Sannino et al., 2022) and as moon dust simulant (Freyria et al., 2019; Manzoli et al., 2021), showing a large potential for further applications. A commercial zeolite A, well known as regards its features, has been selected as starting material for its high cation exchange capacity, due to the Si/Al ratio = 1.00, and for its low cost, due to the large availability. Although various magnetic composites have been previously

synthesized providing a magnetite core to an adsorbent material, employing iron sludge (Wan et al., 2020) or by modification of activated carbon (Guo et al., 2018), no magnetic materials have been so far obtained by exchange of Fe^{2+} ions. This study aims at evaluating the ability of the magnetic nanocomposites in the removal of GA from wastewaters by adsorption, investigating the most relevant physicochemical aspects of the GA adsorption, with particular attention to the main process parameters (solid/liquid ratio, pH, time, initial concentration of GA). A regeneration procedure for the exhausted adsorbent has also been proposed, to ensure the reuse of the magnetic nanoparticles, as well as the recovery of the GA, which is of interest due to its significant commercial value.

2. Materials and Methods

2.1. Materials

Carlo Erba reagent grade synthetic zeolite 4A ($Na_{12}Al_{12}Si_{12}O_{48}\cdot 27H_2O$, framework type LTA, was used in this study. The average grain size is about 8-10 µm~~Its grain size distribution is reported in (~~Marocco et al., 2011). Exchange solutions were prepared dissolving Carlo Erba reagent grade 99.5 wt.% $FeSO_4\cdot 7H_2O$ and NH_4Cl in doubly distilled water. Gallic acid (3,4,5-trihydroxybenzoic acid, 98.0% purity), employed as a bioactive compound, was supplied by Fluka (Bruch, Switzerland).

2.2. Preparation of Gallic Acid solution

GA (25 mg) was dissolved in 10 mL of ultrapure water for 2 h at room temperature under magnetic stirring to obtain a 15 mM solution. It was stored at 4 °C in the dark to avoid oxidation reactions. The stock solution was suitably diluted with ultrapure water to have the following concentrations: 1000, 800, 500, 250, 150, 50 and 10 µM. The analytical determination of GA was carried out by UV-vis spectrophotometer (ThermoScientific Varioskan Flash, Finland) at 265 nm.

2.3. Preparation of metal ceramic nanocomposites

Two magnetic metal-ceramic nanocomposites were prepared starting from zeolite A: ZA1 (labeled as (Fe,H)A800C-0min in previous works (Pansini et al., 2018); ZA2 (labeled as (Fe,H)A600C-90min in previous works (Pansini et al., 2018). In Figure 1 the procedure followed in preparing the metal-ceramic nanocomposites is outlined.

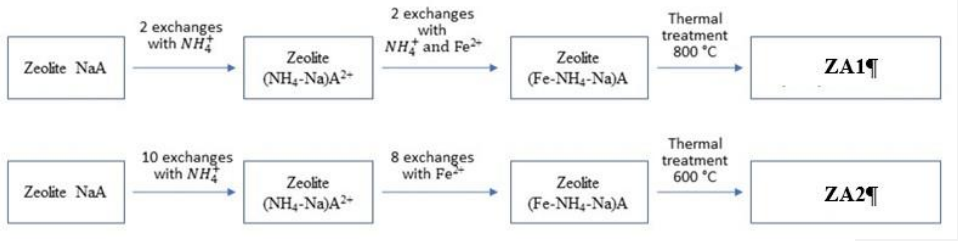

Figure 1. Procedure followed in the preparation of ZA1 and ZA2 magnetic adsorbents.

The magnetic nanocomposite ZA1 was produced as follows. Zeolite A was contacted with a $[NH_4^+]$ = 0.1 M solution at a wt. solid/liquid ratio of (S/L) = 1/50 g/g, room temperature and contact time (t) = 1 h. Then, the solid was separated from the liquid through filtration and contacted again with a fresh solution. This operation was iterated two times. Subsequently, this sample of NH_4^+-exchanged zeolite A was contacted with a $[Fe^{2+}] = [NH_4^+]$ = 0.1 M solution at a wt. solid/liquid ratio of (S/L) = 1/50 and contact time (t) = 1 h. In this exchange the temperature (T) was ≈ 7 °C and Ar was bubbled through the solution to prevent Fe^{2+} oxidation (Weidentaler et al., 2005). The solid particles were separated from the liquid through filtration and contacted again with a fresh solution. This operation was iterated two times. The resulting powders were washed with doubly distilled water, dried for about one day at 80 °C, and stored for at least 3 days in an environment with about 50% relative humidity, to allow water saturation of the zeolite. This sample of NH_4^+ and Fe^{2+} exchanged zeolite A was subjected to the following thermal treatment under a reducing atmosphere (created by a flow of a H_2-Ar gaseous mixture, containing 2 vol. % H_2) in an Al_2O_3 tubular furnace (inner diameter = 6.9 cm, height = 91 cm), using Pt crucibles: heating from room temperature up to 800 °C (15 °C/min heating rate); as soon as the temperature of 800 °C was reached, the heating system of the furnace was switched off and the sample was left to cool down to room temperature within the furnace. The sample ZA2 was produced as

follows. Zeolite A was contacted with a [NH_4^+] = 0.1 M solution according to the same procedures of the previous sample. This exchange was iterated ten times. Then this sample of NH_4^+ exchanged zeolite A was contacted with a [Fe^{2+}] = 0.1 M solution at a wt. solid/liquid ratio of (S/L) = 1/50 g/g, temperature (T) ≈ 7 °C, contact time (t) = 1 h and under Ar bubbling. This operation was iterated eight times. The resulting powders were washed, dried and kept as in the previous case. This sample of NH_4^+ and Fe^{2+} exchanged zeolite A was subjected to the following thermal treatment under a reducing atmosphere: heating from room temperature up to 600 °C (15 °C/min heating rate) and subsequent thermal treatment at 600 °C for 90 min; then, the heating system of the furnace was switched off and the sample was left to cool down to room temperature within the furnace. Samples ZA1 and ZA2 were subjected to X-ray characterization according to what reported in Clayden et al., 2003.

2.4. Characteristics of the nanocomposites

The Fe^{2+} and NH_4^+ exchanged zeolite A undergoes the following phenomena during the thermal treatments under the reducing atmosphere (Colantuono et al., 1997):

1) Shrinkage by dehydration;

2) Evolution of gaseous NH_3, thus leaving hydrogen ions to balance the negative charges of the zeolitic structure, with the formation of acidic Lewis sites;

3) Reduction to Fe^0 or to Fe_3O_4 (with a possible structural damage of the zeolite framework);

4) Migration of the newly formed Fe^0 atoms or Fe_3O_4 particles to form clusters located within the microporous cavities of the zeolite;

5) Migration of the newly formed Fe^0 atoms or Fe_3O_4 particles outside the zeolite cavities to form metallic aggregates at the outer surface of the zeolite grains;

6) Thermal collapse of the zeolite framework;

7) Possible formation of amorphous and other crystalline phases.

The *raison d'être* of the modalities of preparation of the two nanocomposites, clearly explained in detail in ref. (Pansini et al., 2018), are summarized hereafter. Sample ZA1 exhibits a large amount of acidic Lewis sites very useful in adsorption processes and a moderate magnetic response sufficient to perform a magnetic separation

of the solid from the liquid (saturation magnetization M_s = 4.2 emu/g) (Pansini et al., 2018). Sample ZA2 exhibits a strong magnetic response (saturation magnetization M_s = 12.3 emu/g), far more than sufficient to perform a magnetic separation of the solid from the liquid, and a moderate amount of acidic Lewis sites (Pansini et al., 2018). Moreover, a complete chemical, mineralogical, physical characterization of samples ZA1 and ZA2 can be found in the same ref. (Pansini et al., 2018).

2.5. Adsorption experiments

Batch experiments of GA adsorption by magnetic nanocomposites were performed by investigating the following experimental conditions:

- pH. To evaluate the effect of pH, GA adsorption experiments were carried out at solid/liquid (s/l) ratio of 1/100. Actually, 20 mg of adsorbent were contacted with 2 mL of 150 μmol/L GA solution (obtained by diluting 15 mmol/L stock solution) for 2 h, at pH between 3.0 and 8.0. The pH of the solution was properly controlled by addition of either 0.01 or 0.10 mmol/L HCl or NaOH solution. After incubation in a rotatory shaker at 25 °C, the magnetic adsorbents were separated from the liquid using an external magnet (VA03, UNIDISP s.r.l. Italy) and the liquid was analysed to evaluate GA concentration by spectrophotometric analysis. The amount of adsorbed GA was calculated as the difference between the GA quantity initially added and that present in the liquid at equilibrium. Blanks of GA in ultrapure water were analysed in order to check for phenolic compound stability and/or adsorption on the vials.
- Kinetic tests. To evaluate the effect of time on GA adsorption, experiments were performed at solid/liquid ratio 1/100, contacting 20 mg of adsorbent with 2 mL of 150 μmol/L GA solution at pH 5.0 (pH of maximum adsorption). The suspensions were stirred for 0.5, 1.0, 2.0, 3.0, 4.0, 6.0, 24 and 48 h. The longest contact times was that needed to attain equilibrium.
- Adsorption isotherm. The adsorption isotherms were obtained by contacting 20 mg of adsorbent with 2 mL (s/l = 1/100) of GA solution with concentration ranging between 0.01–1000 μmol/L. The pH was kept constant at 5.0 (pH of maximum adsorption) by addition of 0.10 or 0.01 mol/L HCl or NaOH aqueous solution. The

samples were incubated for 24 h (time sufficient to attain equilibrium) and successively subjected to the separation procedure previously described.

2.6 Desorption experiments

The desorption experiments were carried out as follows. 20 mg of adsorbent were contacted with 2 mL (s/l = 1/100) of 200 and 1000 μmol/L GA solution for 24 h, at pH 5.0. Immediately after the end of this GA adsorption step, the solid was separated from the liquid, by using the external magnet, as previously described. Then, the exhausted, GA bearing, adsorbent was contacted with 2 mL of ultrapure water at two different pH values (5.0 and 8.0). After shaking this suspension at 25 °C for 24 h, the adsorbent was magnetically separated from the liquid, and the concentration of the released GA therein was determined.

For each magnetic adsorbent, two desorption cycles were carried out, performing each re-adsorption stage with GA at the same initial concentration (200 and 1000 μmol/L) and at pH 5.0. The concentration of released GA was determined after each desorption stage.

2.7 Thermal analysis

GA was subjected to simultaneous differential thermal analysis (DTA) and thermogravimetric analysis (TG) under inert atmosphere (N_2), using a Perkin-Elmer thermo-analyzer STA 6000, with Al_2O_3 as reference material. The TG and DTA tests were performed keeping 9.00 mg of GA under nitrogen atmosphere, varying the temperature from 30 to 900 °C. A heating rate of 10 °C min^{-1} was adopted.

2.8 FTIR analysis

Fourier transform infrared spectroscopy (FT-IR) spectra were recorded using a Jasco FT–IR 430 spectrophotometer (Jasco Europe, Cremella, Italy). GA, ZA1, ZA2, and GA-complexes, obtained by adsorption of each magnetic adsorbent with GA solution at 1000 μmol/L initial concentration, at pH 5.0 for 24 h at 25 °C, were dried

and ground into a powder form before the FT-IR analyses. Sample powders were mixed in a 1:100 weight ratio with KBr and pressed into a disk under vacuum. The samples were scanned from 400 cm^{-1} to 4,000 cm^{-1}.

3. Results and discussion

3.1. IR Spectra

In order to verify the effective adsorption of GA on the magnetic adsorbents, IR spectra of both the pure GA and the exhausted nanocomposite after GA adsorption were obtained, as shown in the Fig. 2.

The IR spectrum of pure GA shows a shoulder at 3492 cm^{-1} due to the free phenolic O-H stretching and the two bands in the range 3367-3290 attributable to acidic O-H stretching. As expected, the presence of carbonyl group of C=O stretching vibrations is evidenced by the observation of the band at 1703 cm^{-1}, whereas the band at 1618 cm^{-1} appears related to C=C stretching vibration of the aromatic ring, and the band at 791 cm^{-1} can be attributed to δcc benzene ring vibration. Moreover, as reported in literature, the aromatic ring shows two bands at 1541 and 1450 cm^{-1} (Hirun et al., 2012).

The spectra of the exhausted nanocomposites after GA adsorption are composed of combined bands of both GA and each magnetic nanocomposite, demonstrating the presence of adsorbed GA of the surface of nanocomposites. The evidence of this claim is the shift of 3435 cm^{-1} band present in ZA1 to the intense peak at 3413 cm^{-1} observed in the GA-ZA1 nanocomposite on account of the presence of GA. Unlike ZA1 nanocomposite, the shift of the band at 3435 cm^{-1} is not observed in the FTIR spectra of ZA2 and GA-ZA2 nanocomposites. Thus, GA adsorption is denoted solely by the slight increase of the intensity of the peak recorded in the GA-ZA2 spectrum with respect to ZA2 spectrum. This item appears perfectly consistent with the lower amount of GA adsorbed by ZA2 than ZA1 adsorbent (*vide infra*).

a)

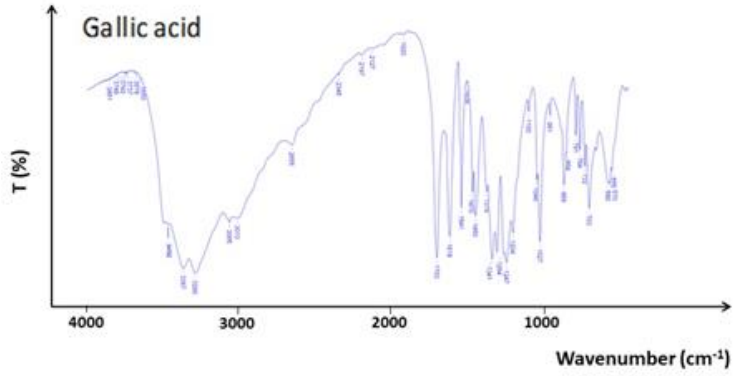

318

319

b)

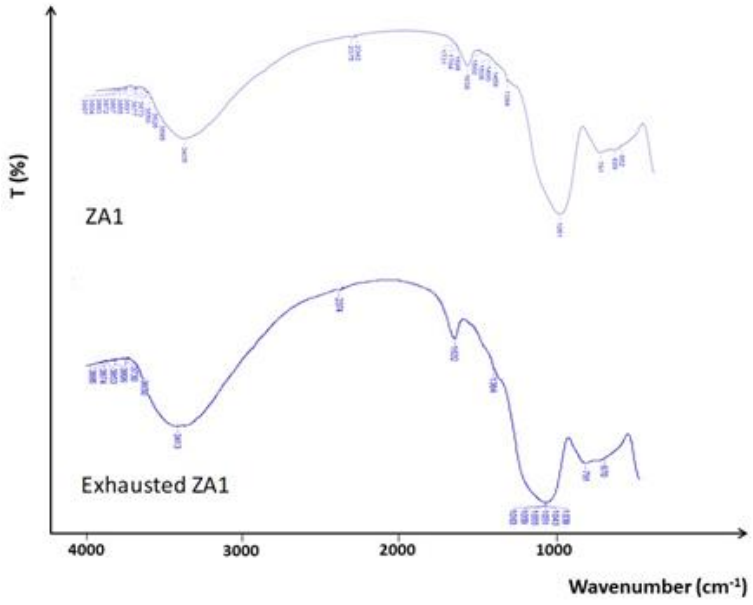

320

321

c)

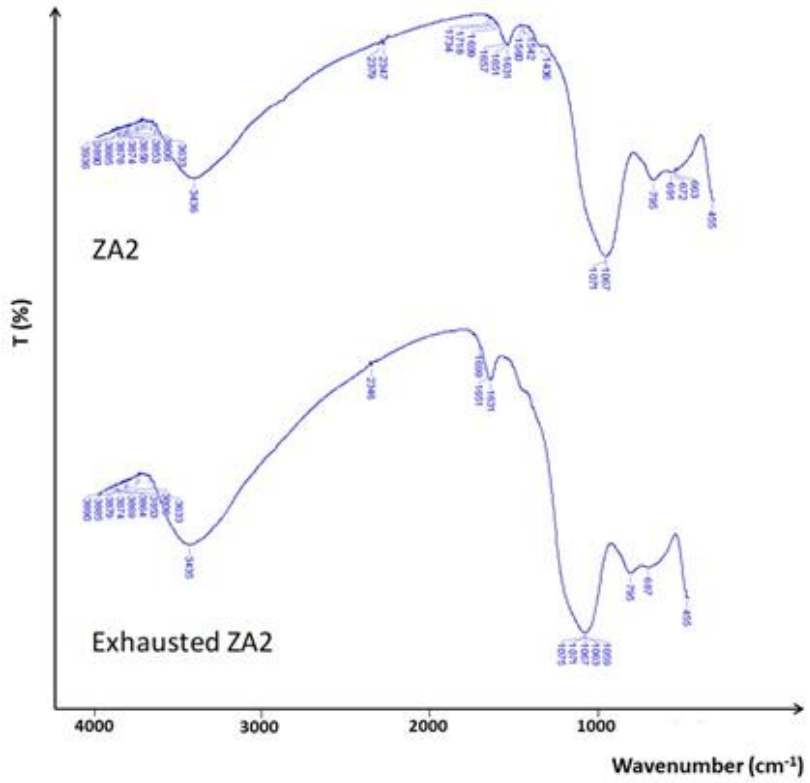

Figure 2. Room-temperature FTIR spectra of (a) pure gallic acid, (b) ZA1 and exhausted ZA1 obtained after gallic acid adsorption, and (c) ZA2 and exhausted ZA2 obtained after gallic acid adsorption.

3.2. Effect of pH on GA adsorption

A set of experiments was carried out to characterize the effect of pH on the adsorption of GA using both the magnetic nanocomposites ZA1 and ZA2. It has been previously shown (Friedman and Jurgens, 2000) that the pH of the medium, as well as the presence of metal ions, may significantly affect the stability and the electronic absorption spectra of polyphenols. As a matter of facts, the pH of the solution may affect not only the surface properties of the adsorbents but also the ionization state of

the adsorbate. The Figure 3 reports the amount of gallic acid adsorbed on the nanocomposites ZA1 and ZA2 as a function of the pH.

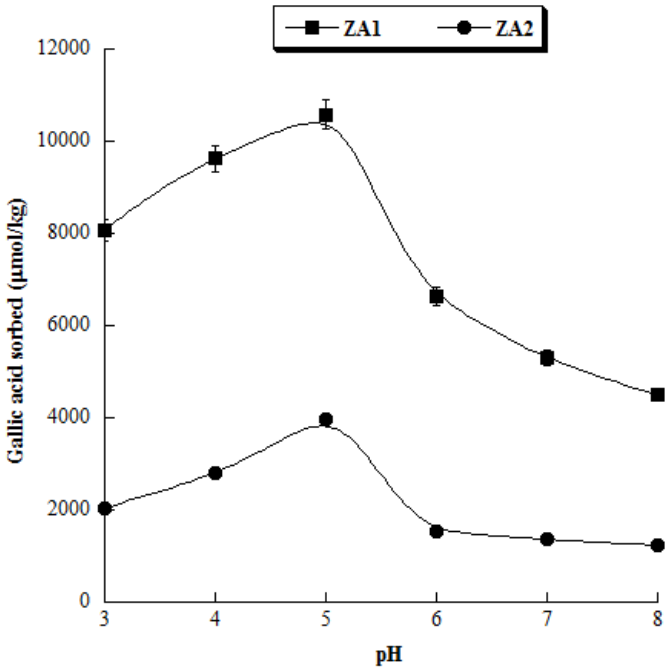

Figure 3. Effect of pH on the adsorption of gallic acid on the magnetic adsorbents ZA1 and ZA2. S/L ratio = 1/100, initial gallic acid concentration = 150 µmol/L, contact time = 2h

Both curves show an adsorption maximum at pH close to 5. The adsorbed amounts of GA are higher in the case of ZA1 (about 10,500 µmol/kg) and lower in the case of ZA2 (about 4,000 µmol/kg). Significant changes in GA uptake were observed when adopting pH values different from the optimum. For both materials, the adsorption of GA significantly increases with increasing pH from 3.0 to 5.0, then it decreases at pH > 5.0, tending towards a horizontal asymptote at pH values higher than 6.0. Consequently, all the subsequent experiments of GA adsorption were carried out at pH=5, corresponding to the maximum adsorption.

In order to explain these results, it is worth observing that the points of zero-charges of ZA1 and ZA2, calculated from ζ-potential curves (Pansini et al., 2018), are 5.6 and 3.7 respectively. As a consequence, when the pH is at the optimum conditions (i.e. close to 5.0), the surface charge of magnetic nanocomposites is close to neutrality.

On the other hand, it is known that GA is a weak polyprotic acid with four acidic protons (the carboxylic group and three phenolic groups), undergoing a pH-dependent deprotonation. Consequently, the distribution between GA and the different gallate anions is affected by the medium pH in a complex way (Jabbari, 2015; Pant et al., 2019). The deprotonation state of GA at a given pH can be expressed in terms of the degree of deprotonation, i.e. the ratio between acidic donated H^+ and total acidic H^+. When the pH is close to 5.0 the degree of deprotonation ratio is about 0.25 (Pant et al., 2018), thus indicating that GA molecules are still mostly protonated (i.e. uncharged).

A similar conclusion can be drawn considering the zero-charge point. Jabbari, 2015 demonstrated that, as the pH increases, a reduction of GA molecular charge is observed, and its molecular charge is zero when the pH is about 6.0. This confirms that, when the pH is close to 5.0, the GA is mostly protonated. Based on the previous considerations, one can argue that adsorption of GA on the nanocomposites may occur through two different mechanisms, on two different locations: i) the silanol groups present on the surface of the nanocomposites; ii) the acidic Lewis sites. As far as the adsorption on silanol groups present on the surface of the nanocomposites is concerned, the pH range around 5.0 represents the only interval in which electrostatic repulsion between the nanocomposites and GA is avoided. Thus, the main interactions occurring between GA and the nanocomposites appear those based on physisorption mechanisms, i.e. π-π interactions, Van der Waals forces, hydrophobic interactions (Zhang et al., 2008). A significant reduction of the adsorption is observed at pH values higher than 6.0, similar to that recorded in previous studies on the adsorption of phenolic compounds on zeolitic materials (Ahmat et al., 2019; Simon et al., 2015). This result can be explained taking into account that the carboxylic acid moiety is completely converted to carboxylate anion, and a significant amount of GA bears two negative charges. These negative charges are stabilized in that the dissociation of orthophenolic OH groups results in the formation of resonant structures, enhancing the conjugation of the original polyphenol ring. Previous studies concerning the GA adsorption on various

adsorbents (Ahmat et al., 2019; Celestino et al., 2019) also indicated the pH as a fundamental factor in the adsorption phenomena due to its impact on both the surface charge of the adsorbent and the ionisation of the adsorbate. In particular, although the adsorbents tested were different, Celestino et al., 2019 observed the maximum adsorption at pH 4-5. On the contrary, Ahmat et al., 2019 in a study focused on the interactions of gallic acid with clay minerals, found that the adsorption was particularly enhanced at pH 2.0 (≈20,000 μmol/kg). In order to explain this result, they made the hypothesis that, at very low pH, the predominance of the protonated form of GA causes a decrease of the repulsion between the neutral GA and Na-montmorillonite. Contemporaneously, the electric charge of clay mineral surface turns cationic, favouring the adsorption of phenolic acids in their anionic form. As under these conditions the GA is almost completely protonated, these authors explained the maximum of GA adsorption at pH = 2.0 with a possible cation exchange process. However, the amount of GA adsorbed turns out to be much lower than that observed with the ZA1 and ZA2 samples, i.e. 70,000 and 60,000 μmol/kg, respectively (*vide infra*, adsorption isotherms). As far as the adsorption on the acidic Lewis sites is concerned, the electron lone pairs of the oxygen atoms of ionized carboxylic groups (about 25 % at pH = 5) interact with the electron hole of the acidic Lewis sites, thus resulting in GA adsorption on the surface of the nanocomposites. Obviously, the removal of ionized GA from water by adsorption, promotes a further GA dissociation and, thus, the concentration of negatively ionized GA molecules in solution remains about constant. Also this kind of adsorption is depressed by pH different from 5.0. Actually: i) the amount of negatively ionized GA is still lower at pHs lower than 5.0; ii) an higher hydroxyl anion concentration preferentially saturates the acidic Lewis sites, being a stronger base than negatively ionized GA molecules, at pHs higher than 5.0. Moreover, adsorption on the acidic Lewis sites explains the higher extent to which adsorption occurs on ZA1 (bearing a far higher number of acidic Lewis sites) than on ZA2 (bearing a far lower number of acidic Lewis sites).

3.3. Adsorption kinetic

The kinetics features of GA (148 μmol/L initial added concentration) uptake from water by ZA1 and ZA2, (S/L ratio=1/100) at pH 5.0 are described in Figure 4.

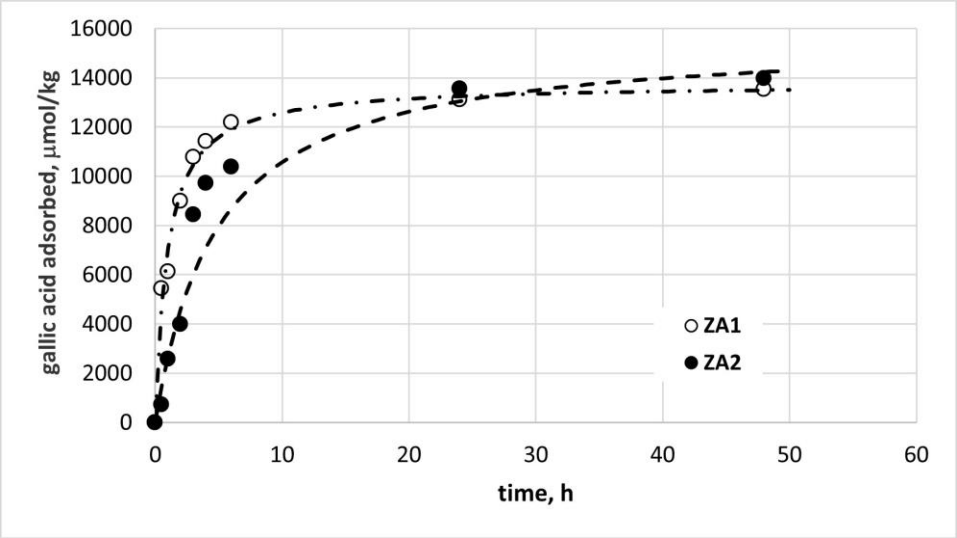

Figure 4. Adsorption kinetics of gallic acid uptake on the magnetic adsorbents ZA1 and ZA2. S/L ratio = 1/100, pH 5.0, initial gallic acid concentration = 150 μmol/L.

The experimental data show an initial sharp increase of the adsorbed amount, followed by a progressive slow down and, after about 24 h, an equilibrium condition. The initial adsorption rate (i.e. the slope of the linear portion of the curves) of ZA1 is faster in comparison to ZA2, (14,700 μmol/(kg h) and 2,350 μmol/(kg h), respectively) although the amounts of GA adsorbed at equilibrium are substantially similar. The asymptotic level reached after 24 h from the curves in Fig. 4 (about 13,000 μmol/kg) were considered as equilibrium values in the subsequent tests.

The experimental curves were best-fitted by the pseudo-second order kinetic model, that has been widely adopted for the adsorption of phenolic compounds in liquid-phase (Wu et al., 2009):

$$\frac{t}{q_t} = \frac{1}{k_2 \cdot q_e^2} + \frac{t}{q_e} \qquad (1)$$

where q_e and q_t are the sorption capacity (expressed in μmol/kg) at equilibrium and at time t, respectively. The parameter k_2, expressed in kg/(μmol min), is the overall rate constant of pseudo second order sorption. The estimates of the parameters included in the model (1), obtained by nonlinear regression, are reported in the Table 1.

Table 1

Estimates of the parameters included in the pseudo-second order model (1).

	ZA1	ZA2
q_e, μmol/kg	13,760	15,660
k_2 kg/μmol min	1.07	0.208

Other authors showed that the adsorption kinetic of gallic acid onto magnetic ion exchange resin (Ding et al., 2020) and on other adsorbents such as arginine-modified magnetic chitosan (AMCS) (Chai et al., 2020), fitted well with the pseudo second-order model.

3.4 Adsorption isotherms

The adsorption isotherms for both the magnetic nanocomposites ZA1 and ZA2 are reported in Figure 5 in terms of adsorbed amounts of each nanocomposite after a 24 h incubation time as a function of GA concentration. The sigmoidal behaviour of the curves shown by both materials suggests V type isotherms. Such isotherms are usually adopted to describe the capillary condensation during the pore filling of micropores, and cover the adsorption of water on hydrophobic microporous solids such as zeolite-analogue materials (Kohler et al., 2017), as well as mesoporous materials.

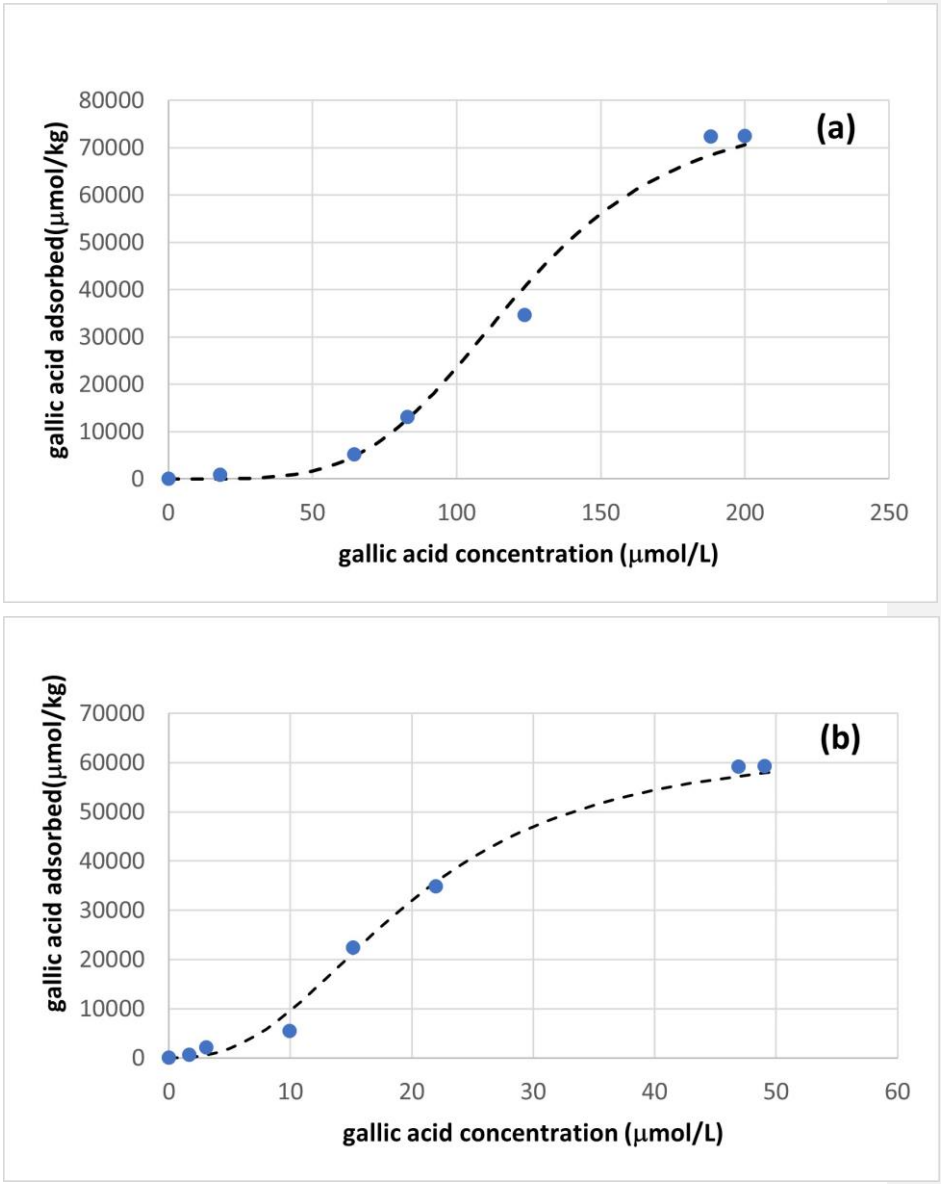

Figure 5. Adsorption isotherms of gallic acid on the magnetic adsorbents ZA1 (a) and ZA2 (b).

The experimental curves have been fitted using the model of Sips, that has been previously adopted for the adsorption of phenolic compounds in liquid-phase (Leitão and Serrao, 2005; Carvajal-Bernal et al., 2017):

$$q_t = \frac{q_m (K_s \cdot C_e)^{\frac{1}{m}}}{1+(K_s \cdot C_e)^{\frac{1}{m}}} \quad (2)$$

where C_e is the equilibrium concentration of gallic acid, q_t is the sorption capacity of the zeolite (expressed in μmol/kg) at equilibrium. q_m (μmol/kg) is the maximum amount of GA adsorbed per unit mass of magnetic nanocomposite, K_s (L/μmol) is the Sips constant related to energy of adsorption, and the parameter m could be regarded as the parameter characterizing the system heterogeneity.

The Sips isotherm model is a combination of the Langmuir and Freundlich isotherm type models and expected to describe heterogeneous surface much better. At low adsorbate concentrations, the Sips isotherm approaches the Freundlich isotherm, whereas it approaches the Langmuir isotherm at high concentrations. The estimates of the parameters included in the model (2) are reported in the Table 2.

Table 2

Estimates of the parameters included in the Sips model (2).

	ZA1	ZA2
q_m, μmol/kg	79,100	64,200
K_s, L/μmol	0.0082	0.051
m, -	0.23	0.40

3.5 Desorption and recycle of the adsorbent

The regeneration and the reuse of the adsorbents play a crucial role in the economical balance of an adsorption process, as they can save resources improving the utilization efficiency. In this view, different desorption procedures were tested. First, to develop an efficient procedure for the thermal regeneration of the exhausted adsorbents,

TGA and DTA analyses were carried on pure GA as well as on both ZA1 and ZA2 nanocomposites. The thermal analysis of GA (Figure 6a) showed a sharp endothermic peak at about 270°C that can be reasonably ascribed to its thermal decomposition. This hypothesis was confirmed by the TGA curve (Figure 6b), showing a sharp mass loss (65% of the total) in the range 270-330°C.

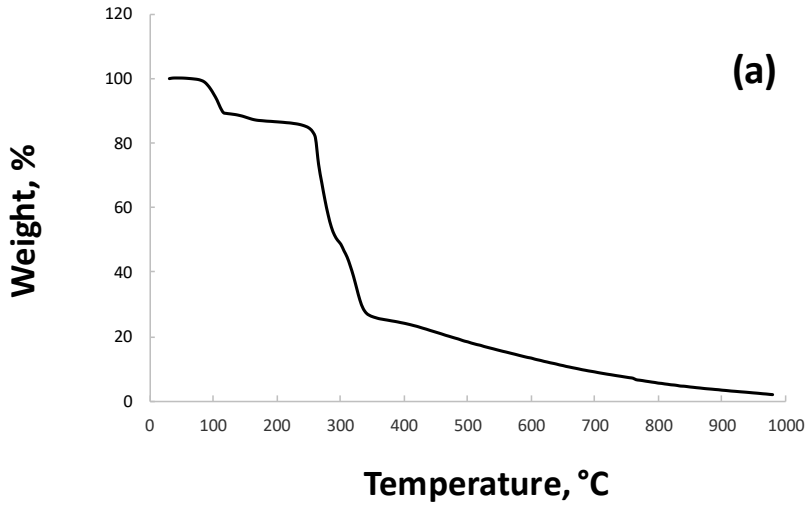

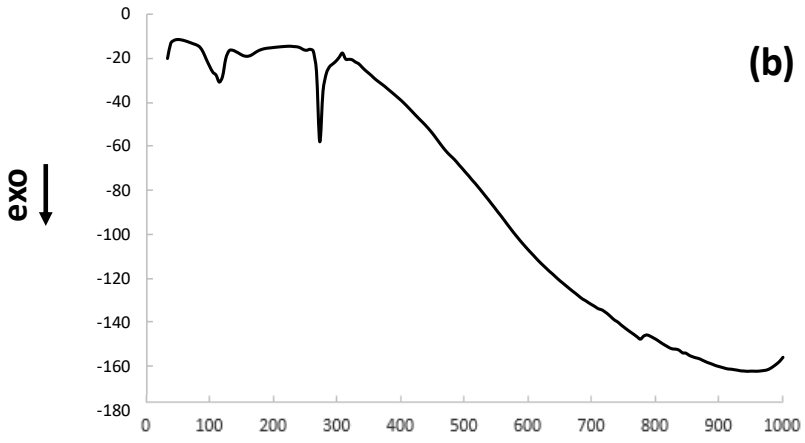

Figure 6. DTA curve (a) and TG curve (b) of gallic acid.

These results indicate that a thermal regeneration of the exhausted adsorbents can be carried out by thermally treating the exhausted, GA bearing, adsorbents, at about 300°C under an inert atmosphere, to avoid the oxidation of Fe^0 or Fe_3O_4 nanoparticles. On the other hands, the TGA and DTA curves of ZA1 and ZA2 demonstrate high thermal and chemical stability of the adsorbents at temperatures far higher than 300°C. In order to find a more environmentally friendly strategy and to recover the GA, a desorption procedure based on pH changes, as described in the Materials and Methods section, was then attempted. The desorption procedure was fully unsuccessful at pH 5, demonstrating that at this value of pH the adsorption equilibrium is completely shifted towards the adsorbed phase (data not shown). On the contrary, when carrying out the desorption at pH 8, the results were much more satisfactory. The results shown in the Figure 7 demonstrate that a complete regeneration was obtained after the second desorption cycle, whatever the initial concentration of GA adopted (200 μmol/L and 1000 μmol/L) and the nanocomposite used (ZA1 and ZA2). These results confirmed the strong dependence of the adsorption of GA on ZA1 and ZA2 on pH, as previously evidenced (*vide supra*).

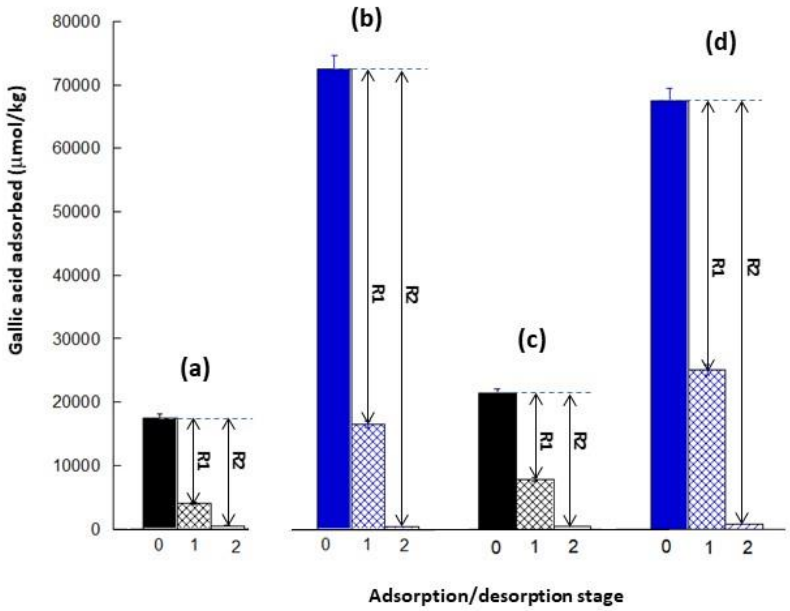

514

515 **Figure 7**. Regeneration of the exhausted adsorbent at pH 8 under different operating
516 conditions:
517 (a): adsorbent ZA1, initial concentration: 200 µmol/L, pH 8
518 (b): adsorbent ZA1, initial concentration: 1000 µmol/L, pH 8
519 (c): adsorbent ZA2, initial concentration: 200 µmol/L, pH 8
520 (d): adsorbent ZA2, initial concentration: 1000 µmol/L, pH 8
521 Rectangles:
522 0 – gallic acid adsorbed before desorption
523 1 – residual GA adsorbed after the first desorption stage
524 2 – residual GA adsorbed after the second desorption stage
525 Arrows:
526 R1: Amount of GA released during the first desorption stage
527 R2: Amount of GA released during the first two desorption stages
528
529

4. Conclusions

The adsorption of GA, a toxic pollutant increasingly found in wastewaters from food and pharmaceutical industries, has been efficiently carried out using two tailor-made magnetic metal-ceramic nanocomposites, obtained from zeolite A (ZA1 and ZA2). The nanocomposites have been developed by a cation-exchange treatment followed by a thermal treatment at relatively moderate temperatures under reducing atmosphere. The efficiency of the magnetic adsorbents strongly depends on pH, with a maximum in the pH range around 5.0. In this interval the two different modalities of GA adsorption on ZA1 and ZA2 attain their maximum for different reasons previously explained.

The adsorption kinetics is described by the pseudo-second order model. The equilibrium isotherms were satisfactorily described by the Sips model, a combination of the Langmuir and Freundlich isotherm type models. Specific tests were carried out to develop a procedure for the regeneration of exhausted adsorbents. First, a thermal regeneration procedure was developed on the basis of the results of DT and TGA analyses. In order to offer a more environmentally friendly, an alkaline desorption was carried out, obtaining the complete regeneration of the magnetic adsorbents and recover of GA. The results obtained demonstrate that magnetic metal-ceramic nanocomposites obtained from zeolites offer a technically and economically feasible method to remove GA from wastewaters, ensuring environmental sustainability, multicycle regenerability of the adsorbents, and the recovery of the economically valuable product.

CRediT authorship contribution statement

Domenico Pirozzi: Data curation, Writing – original draft. **Michele Pansini**: Writing/review and editing. **Antonello Marocco**: Investigation; Methodology. **Serena Esposito**: Visualization, Writing - review & editing. **Gabriele Barrera**: Investigation; Methodology. **Paola Tiberto**: Investigation; Methodology. **Paolo Allia**: Investigation; Methodology. **Filomena Sannino**: Supervision, Writing – original draft.

Declaration of Competing Interest

The authors declare that they have no known competing financial interests or personal relationships that could have appeared to influence the work reported in this paper.

Funding: This research received no external funding.

References

Addorisio, V., Esposito, S., Sannino, F., 2010. Sorption capacity of mesoporous metal oxides for the removal of MCPA from polluted waters. J. Agric. Food Chem. 58, 5011-5016.

Addorisio, V., Pirozzi, D., Esposito, S., Sannino, F., 2011. Decontamination of waters polluted with simazine by sorption on mesoporous metal oxides. J. Hazard. Mater. 196, 242-247.

Ahmat, A.M., Thiebault, T., Guégan, R., 2019. Phenolic acids interactions with clay minerals: A spotlight on the adsorption mechanisms of gallic acid onto montmorillonite. Appl. Clay Sci. 180, 105188, https://doi.org/10.1016/j.clay.2019.105188.

Al Zahrani, N.A., El-Shishtawy, R.M., Asiri, A.M., 2020. Recent developments of gallic acid derivatives and their hybrids in medicinal chemistry: A review. Eur. J. Med. Chem. 204, 112609, https://doi.org/10.1016/j.ejmech.2020.112609.

Badhani, B., Sharma, N., Kakkar, R., 2015. Gallic acid: a versatile antioxidant with promising therapeutic and industrial applications. RSC Adv. 5, 27540-27557, https://doi.org/10.1039/C5RA01911G.

Carvajal-Bernal, A.M., Gomez-Granados, F., Giraldo, L., Moreno-Pirajan, J.C., 2017. Application of the Sips model to the calculation of maximum adsorption capacity and immersion enthalpy of phenol aqueous solutions on activated carbons. Chem. Eur. J. 8, 112-118.

Celestino, G.G., Henriques, R.R., Shiguihara, A.L., Constantino, V.R.L., de Siqueira Melo, R., Amim Júnior, J., 2019. Adsorption of gallic acid on nanoclay modified with poly(diallyldimethylammonium chloride). Environ. Sci. Pollut. Res. Int., 26(28), 28444-28454.

Chai, Z., Li, C., Zhu, Y., Song, X., Chen, M., Yang, Y., Chen, D., Liang, X., Wu, J., 2020. Arginine-modified magnetic chitosan: Preparation, characterization and adsorption of gallic acid in sugar solution. Int. J. Biol. Macromol. 165, 506-516.

Clayden, E., Esposito, S., Ferone, C., Pansini, M., 2003. ^{27}Al and ^{28}Si NMR study of the thermal transformation of Ba-exchanged zeolite A into monoclinic celsian. J. Mat. Chem. 13, 1681-1685.

Colantuono, A., Dal Vecchio, S., Mascolo, G., Pansini, M., 1997. Thermal shrinkage of various cation forms of zeolite A. Thermochim. Acta 296, 59-66.

Di Martino, M., Sannino, F., Pirozzi, D., 2015. Removal of pesticide from wastewater: Contact time optimization for a two-stage batch stirred adsorber. J. Environ. Chem. Eng. 3, 365-372.

Ding, L., Guo, C., Zhu, Y., Ma, J., Kong, Y., Zhong, M., Cao, Q., Zhang, H., 2020. Adsorptive removal of gallic acid from aqueous solution onto magnetic ion exchange resin. Water Sci. Technol. 81, 1479-1493.

Esposito, S., Dell'Agli, G., Marocco, A., Bonelli, B., Allia, P., Tiberto, P., Barrera, G., Manzoli, M., Arletti, R., Pansini, M., 2018. Magnetic metal-ceramic nanocomposites obtained from cation-exchanged zeolite by heat treatment in reducing atmosphere. Microporous Mesoporous Mater. 268, 131-143.

Esposito, S., Marocco, A., Bonelli, B., Pansini, M., 2015. PCT international application published under Number WO2015/145230 A1.

Esposito, S., Marocco, A., Dell'Agli, G., Bonelli, B., Mannu, F., Allia, P., Tiberto, P., Barrera, G., Pansini, M., 2020. Separation of biological entities from human blood

by using magnetic nanocomposites obtained from zeolite precursors. Molecules 25, 1803 ~~1820~~ https://doi:10.3390/molecules25081803.

Esposito, S., Pansini, M., Bonelli, B., Garrone, E., 2013. Modes of interaction of simazine with the surface of model amorphous silica in water. J. Phys. Chem. 117 (21), 11203-11210.

Freyria, F.S., Marocco, A., Esposito, S., Bonelli, B., Barrera, G., Tiberto, P., Allia, P., Oudayer, P., Roggero, A., Matéo-Vélez, J.C., Dantras, E., Pansini, M., 2019. Simulated moon agglutinates obtained from zeolite precursor by means of a low-cost and scalable synthesis method. ACS Earth Sp. Chem. 3 (9), 1884-1895.

Friedman, M., Jürgens, H.S., 2000. Effect of pH on the stability of plant phenolic compounds. J. Agric. Food Chem. 48, 2101-2110.

Guo, F.Q., Li, X.L., Jiang, X.C., Zhao, X.M., Guo, C.L., Rao, Z.H., 2018. Characteristics and toxic dye adsorption of magnetic activated carbon prepared from biomass waste by modified one-step synthesis. Colloids Surf. A Physicochem. Eng. Asp. 555, 43-54.

Hirun, N., Dokmaisrijan, S., Tantishaiyakul, V., 2012. Experimental FTIR and theoretical studies of gallic acid–acetonitrile clusters. Spectrochim. Acta A 86, 93-100.

Hsieh, C.L., Lin, C.H., Wang, H.E., Peng, C.C., Peng, R.Y., 2015. Gallic acid exhibits risks of inducing muscular hemorrhagic liposis and cerebral hemorrhage—its action mechanism and preventive strategy. Phytother. Res. 29, 267-280.

Jabbari, M., 2015. Solvent dependence of protonation equilibria for gallic acid in water and different acetonitrile–water cosolvent systems. J. Mol. Liq. 208, 5-10.

Kohler, T., Hinze, M., Müller, K., Schwieger, W., 2017. Temperature independent description of water adsorption on zeo-types showing a type V adsorption isotherm. Energy 135, 227-236.

Leitão, A., Serrão, R., 2005. Adsorption of phenolic compounds from water on activated carbon: prediction of multicomponent equilibrium isotherms using single-component data. Adsorption 11, 167-179.

Lu, Z.B., Nie, G.J., Belton, P.S., Tang, H.R., Zhao, B.L., 2006. Structure-activity relationship analysis of antioxidant ability and neuroprotective effect of gallic acid derivatives. Neurochem. Int. 48, 263-274.

Manzoli, M., Tammaro, O., Marocco, A., Bonelli, B., Barrera, G., Tiberto, P., Allia, P., Matéo-Vélez, J.C., Roggero, A., Dantras, E., Arletti, R., Pansini, M., Esposito, S., 2021. New insight in the production of simulated moon agglutinates: the use of natural zeolite-bearing rocks. ACS Earth Sp. Chem. 5 (6), 1631-1646.

Marocco, A., Dell'Agli, G., Pansini, M., Sannino, F., Allia, P., Tiberto, P., Barrera, G., Esposito, S., ~~2019~~2020. Removal of agrochemcals from water by adsorption: a critical comparison among humic-like substances, zeolites, porous oxides, and magnetic nanocomposites. Processes 8, 141-167.

Marocco, A., Liguori, B., Dell'Agli, G., ~~Bonelli, B~~., Pansini, M., 2011. Sintering behavior of celsian based ceramics obtained from the thermal transformation of Ba-exchanged zeolite A into monoclinic celsian. J. Eur. Ceram. Soc. 31, 1965-1973.

Moreno-Álvarez, S.A., Martínez-Castañón, G.A., Niño-Martínez, N., Reyes-Macías, J.F., Patiño-Marín, N., Loyola-Rodríguez, J.P., Ruiz, F., 2010. Preparation and bactericide activity of gallic acid stabilized gold nanoparticles, J. Nanopart. Res. 12, 2741-2746.

Commentato [ES1]: Non è un inizio pagina ma un numero identificativo

Pansini, M., Dell'Agli, G., Marocco, A., Netti, P.A., Battista, E., Lettera, V., Vergara, P., Allia, P., Bonelli, B., Tiberto, P., Barrera, G., Martra, G., Arletti, R., Esposito, S., 2017. Preparation and characterization of porous metal-ceramic nanocomposites from a zeolite precursor and their application for DNA separation. J. Biomed. Nanotechnol. 13 (3), 337-348.

Pansini M., Sannino, F., Marocco, A., Allia, P.M., Tiberto, P., Barrera, G., Polisi, M., Battista, E., Netti, P., Esposito, S., 2018. Novel process to prepare magnetic metal-ceramic nanocomposites from zeolite precursor and their use as adsorbent of agrochemicals from water. J. Environ. Chem. Eng. 6 (1), 527-538.

Pant, A.F., Özkasikci, D., Fürtauer, S., Reinelt, M., 2019. The effect of deprotonation on the reaction kinetics of an oxygen scavenger based on gallic acid. Front. Chem. 7, 680-686.

Pasanphan, W., Buettner, G.R., Chirachanchai, S., 2010. Chitosan gallate as a novel potential polysaccharide antioxidant: an EPR study. Carbohydr. Res. 345, 132-140.

Pirozzi D., Sannino F., 2014. Design of a multi-stage stirred adsorber using mesoporous metal oxides for herbicide removal from wastewaters. J. Environ. Chem. Eng. 2, 211-219.

Sannino, F., Pansini, M., Marocco, A., Cinquegrana, A., Esposito, S., Tammaro, O., Barrera, G., Tiberto, P., Allia, P., Pirozzi, D., 2022. Removal of sulfanilamide by tailor-made metal-ceramic nanocomposite adsorbents. J. Environ. Manag. 310, 114701-~~114709~~.

Sannino, F., Ruocco, S., Marocco, A., Esposito, S., Pansini, M., 2012. Cyclic process of simazine removal from waters by adsorption on zeolite H-Y and its regeneration by thermal treatment~~Simazine removal from waters by adsorption on zeolite H-Y and its regeneration by thermal treatment~~. J. Hazard. Mat. 229-230, 354-360.

Sannino, F., Ruocco, S., Marocco, A., Esposito, S., Pansini, M., 2013. Simazine removal from waters by adsorption on porous silica tailored by the sol-gel technique. Micr. Mes. Mat. 180, 178-186.

Simon, V., Thuret, A., Candy, L., Bassil, S., Duthen, S., Raynaud, C., Masseron, A., 2015. Recovery of hydroxycinnamic acids from renewable resources by adsorption on zeolites, Chem. Eng. J. 280, 748-754.

Sousa, A.M.L., Li, T.D., Varghese, S., Halling, P.J., Lau, K.H.A., 2018. Highly active protein surfaces enabled by plant-based polyphenol coatings. ACS Appl. Mater. Interfaces 10, 39353-39362.

Srivastava, B., Jhelum, V., Basu, D.D., Patanjali, P.K. 2009. Adsorbents for pesticide uptake from contaminated water: a review. J. Sci. Ind. Res. 68, 839-850.

Wan, J., Ding, J., Tan, W., Gao, Y., Sun, S., He, C., 2020. Magnetic-activated carbon composites derived from iron sludge and biological sludge for sulfonamide antibiotic removal. Environ. Sci. Poll. Res. 27, 13436-13446.

Weidentaler, C., Zibrovius, B., Schimanke, J., Mao, Y., Mienert, B., Schmidt, W., 2005. Behavior of ferrous cations during ion exchange into zeolites under atmospheric conditions. Micr. Mes. Mat. 84, 302-317.

Wu, F.C., Tseng, R.L., Huang, S.C., Juang, R.S., 2009. Characteristics of pseudo-second-order kinetic model for liquid-phase adsorption: A mini-review. Chem. Eng. J. 151, 1-9.

Yang, W., Ding, H., Qi, G., Li, C., Xu, P., Zheng, T., Zhu, X., Kenny, J.M., Puglia, D., Ma, P., 2021. Highly transparent PVA/nanolignin composite films with excellent

Commentato [ES2]: Non è un inizio pagina ma un numero identificativo

746 UV shielding, antibacterial and antioxidant performance. React. Funct. Polym.
747 162, 104873-104882.
748 Zhang, Y., Dong, L., Li, J., Chen, X., 2008. Studies on the interaction of gallic acid with
749 human serum albumin in membrane mimetic environments. Talanta, 76, 246-253.
750 Zhang, Z, Pang, Q, Li, M, Zheng, H, Chen, H, Chen, K, 2015. Optimization of the
751 condition for adsorption of gallic acid by *Aspergillus oryzae* mycelia using Box-
752 Behnken design. Environ Sci Pollut Res, 22, 1085-1094.
753 Zheng, M., Zhang, C., Zhou, Y., Lu, Z., Zhao, H., Bie, X., Lu, F., 2018. Preparation of
754 gallic acid-grafted chitosan using recombinant bacterial laccase and its application
755 in chilled meat preservation. Front. Microbiol. 9, 1729-1738.
756
757